Mutation Research 726 (2011) 129–135

Contents lists available at SciVerse ScienceDirect

Mutation Research/Genetic Toxicology and Environmental Mutagenesis

journal homepage: www.elsevier.com/locate/gentox
Community address: www.elsevier.com/locate/mutres

Genotoxic effects of silver nanoparticles stimulated by oxidative stress in human normal bronchial epithelial (BEAS-2B) cells

Ha Ryong Kim[c], Mi Jie Kim[c], Soo Yeun Lee[a], Seung Min Oh[b,**,1], Kyu Hyuck Chung[c,*,1]

[a] College of Pharmacy, Keimyung University, 1000, Sindang-dong, Dalseo-gu, Daegu 704-701, South Korea
[b] Hoseo Toxicological Research Center, Hoseo University, 165, Sechul-ri, Baebang-myun, Asan, Chungnam 336-795, South Korea
[c] School of Pharmacy, Sungkyunkwan University, 300, Cheoncheon-dong, Jangan-gu, Suwon, Gyeonggi-do 440-746, South Korea

ARTICLE INFO

Article history:
Received 5 May 2011
Received in revised form 22 July 2011
Accepted 26 August 2011
Available online 17 September 2011

Keywords:
Silver nanoparticles
Genotoxicity
Oxidative stress
BEAS-2B cells

ABSTRACT

Many classes of silver nanoparticles (Ag-NPs) have been synthesized and widely applied, but the genotoxicity of Ag-NPs and the factors leading to genotoxicity remain unknown. Therefore, the purpose of this study is to elucidate the genotoxic effects of Ag-NPs in lung and the role of oxidative stress on the genotoxic effects of Ag-NPs. For this, Ag-NPs were completely dispersed in medium by sonication and filtration. The Ag-NPs dispersed in medium were 43–260 nm in size. We observed distinct uptake of Ag-NPs into BEAS-2B cells. The Ag-NPs aggregates were wrapped with an endocytic vesicle within the cytoplasm and nucleus of BEAS-2B cells. In the comet assay and micronucleus (MN) assay for BEAS-2B cells, Ag-NPs stimulated DNA breakage and MN formation in a dose-dependent manner. The genotoxic effect of Ag-NPs was partially blocked by scavengers. In particular, of the scavengers tested, superoxide dismutase most significantly blocked the genotoxic effects in both the cytokinesis-block MN assay and the comet assay. In the modified comet assay, Ag-NPs induced a significant increase in oxidative DNA damage. Furthermore, in the oxidative stress assay, Ag-NPs significantly increased the reactive oxygen radicals. These results suggest that Ag-NPs have genotoxic effects in BEAS-2B cells and that oxidative stress stimulated by Ag-NPs may be an important factor in their genotoxic effects.

1. Introduction

Nanomaterials are defined by the U.S. National Nanotechnology Initiative as materials that are 1–100 nm in size in at least one dimension. In recent years, nanotechnology has been involved in the creation and manipulation of materials at nanoscale levels to generate products that exhibit novel properties [1]. In particular, nanoparticles have been proposed for the treatment of many diseases that require a constant drug concentration in the blood or specific drug targeting of cells or organs [2,3]. With the development of nanotechnology, the size effects of particles have gradually been considered to be important. However, although the novel properties of nanomaterials are impressive from a physicochemical viewpoint, there are concerns about their possible adverse effects on biological systems. Nanoparticles may be more toxic than larger particles of the same substance because of their larger surface area and enhanced chemical reactivity [4]. Moreover, some nanoparticles readily travel throughout the body, deposit in target organs, penetrate cell membranes, lodge in mitochondria, and may trigger injurious responses [5–7].

Silver (Ag) is a naturally occurring element that has been widely used for thousands of years in applications such as jewellery, utensils, monetary currency, dental alloys, photography, and even explosives [8]. In addition, Ag is widely known as a catalyst, oxidizing methanol to formaldehyde and ethylene to ethylene oxide [9]. Strong growth is projected in the silver nanoparticles (Ag-NPs) market in the coming years [10]. This increasing use of Ag-NPs necessitated a health and environmental risk assessment [10,11]. In particular, because pulmonary exposure to Ag-NPs occurs during handling of Ag-NPs, it was necessary to evaluate the toxic response in the respiratory tract. The results of 90-day inhalation studies with Ag-NPs indicated that lungs and liver are the major target tissues for Ag-NPs accumulation [12,13]. It was recently reported that exposure of human lung epithelial cells to metal-containing nanoparticles generated reactive oxygen species (ROS), which can lead to oxidative stress and cellular damage [14]. Barillet et al. [15] reported that silicon carbide nanoparticles induced genotoxicity and oxidative stress in A549 lung epithelial cells. In addition, Kim et al. [16] reported that Ag-NPs induced oxidative stress-dependent toxicity in human liver cells. However, there is no report on the genotoxic effects of Ag-NPs or the role of oxidative stress in these

* Corresponding author. Tel.: +82 31 290 7714; fax: +82 31 290 7771.
** Corresponding author. Tel.: +82 41 540 9697; fax: +82 41 540 9697.
E-mail addresses: ohsm0403@hoseo.edu (S.M. Oh), khchung@skku.edu (K.H. Chung).
[1] S.M. Oh and K.H. Chung contributed equally.

1383-5718/$ – see front matter © 2011 Elsevier B.V. All rights reserved.
doi:10.1016/j.mrgentox.2011.08.008

effects in normal lung epithelial cells. Therefore, we examined the genotoxic potential of Ag-NPs and the role of oxidative stress in their effects in a human normal bronchial epithelial (BEAS-2B) cell line.

We purchased Ag nanopowder (<100 nm) and completely dispersed them in experimental medium by sonication. After this process, the Ag-NPs solution was filtrated using a membrane filter; the Ag-NPs were then physically characterized. First, prior to their genotoxic evaluation, the uptake of Ag-NPs was characterized along with their effects on cellular adhesion and their surface distribution. Second, in order to evaluate the genotoxic potential of Ag-NPs in human pulmonary exposure, cultured human lung cells (BEAS-2B cells) were used in the comet assay and the *in vitro* micronucleus (MN) assay. Third, we identified the genetic toxicity related to ROS generation by Ag-NPs. To measure ROS generation, an oxidative stress assay of intracellular oxidation of 2′,7′-dichlorofluorescein-diacetate (DCFH-DA) was performed [1,17]. In addition, specific bacterial enzymes, formamidopyrimidine DNA glycosylase (FPG) and endonuclease III (Endo III), were used to measure oxidized purine and oxidized pyrimidine in the modified comet assay (Comet assay interest group website; http://cometassay.com/). To determine whether the genotoxic effect of Ag-NPs was stimulated by ROS, BEAS-2B cells were co-treated with both Ag-NPs (10 μg/ml) and scavengers [mannitol (Man), OH radical scavenger; catalase (CAT) and sodium selenite (SS), H_2O_2 radical scavengers; superoxide dismutase (SOD), superoxide radical scavenger] in the comet assay and the cytokinesis-block MN (CBMN) assay.

2. Materials and methods

2.1. Ag-NPs preparation

Ag-NPs (Sigma–Aldrich, St. Louis, MO, USA) were homogenously dispersed in bronchial-epithelial growth medium (BEGM; Clonetics Corp., Walkersville, MD, USA) by sonication for 30 min (Bioruptor UCD-200T, Cosmobio Corp., Japan), and filtered through a cellulose membrane (pore size 200 nm, Advantec, Toyo Toshi Kaisha, Japan). Ag-NPs were serially diluted to 0.01, 0.1, 1, and 10 μg/ml and incubated with the BEAS-2B cell line.

2.2. Characterization of Ag-NPs

The size and shape of Ag-NPs were characterized by using a scanning electron microscope (SEM; Jeol JSM 7000F, Tokyo, Japan) and a transmission electron microscope (TEM; Jeol JEM 2100F, Tokyo, Japan). Ag-NPs were coated with platinum/palladium (Pt/Pd) and then viewed using SEM. Also, one drop of Ag-NP suspension was dried onto a 400-mesh carbon-coated copper grid and imaged with a TEM at 200 kV. The size distribution of Ag-NPs was evaluated using dynamic light scattering (DLS) on the ELSZ-2 (Otsuka Electronics Co., Inc., Osaka, Japan).

2.3. Cell culture

The BEAS-2B cell line (normal human lung bronchial epithelial cells) was obtained from the ATCC (American Type Culture Collection). The BEAS-2B cells were grown in BEGM supplemented with 0.5 ng/ml recombinant epidermal growth factor (EGF), 500 ng/ml hydrocortisone, 0.005 mg/ml insulin, 0.035 mg/ml bovine pituitary extract, 500 nM ethanolamine, 500 nM phosphoethanolamine, 0.1 ng/ml transferring, 6.5 ng/ml 3,3,5-triiodothyronine, 500 ng/ml epinephrine, 0.1 ng/ml retinoic acid, penicillin (100 units/ml) and streptomycin (100 μg/ml) at 37 °C in an atmosphere of 5% CO_2/95% air under saturating humidity. The cells were treated with various concentrations of Ag-NPs as described in the toxicological study.

2.4. Intracellular localization of Ag-NPs

Ag-NP-treated BEAS-2B cells were collected using 2.5% trypsin–EDTA, fixed in 2% glutaraldehyde in cacodylate buffer, pH 7.2, and post-fixed in 1% osmium tetroxide. The cells were dehydrated in graded concentrations of ethanol and embedded in Spurr's resin. The 80 nm sections of the embedded cells were observed with TEM (Jeol JEM 1010, Tokyo, Japan) at 40–100 kV.

2.5. In vitro comet assay

To evaluate the DNA damage by Ag-NPs in BEAS-2B cells, we performed the comet assay as described by Singh et al. [18]. The BEAS-2B cells were added to a 12-well plate and the culture was maintained at 37 °C in a 5% CO_2 atmosphere. After 24 h incubation, the cells were exposed to Ag-NPs only or Ag-NPs with scavengers (Man 0.5 μM, SS 1 μg/ml, CAT 2 units/ml, and SOD 30 units/ml) for 24 h [19–22]. The treated cells were then trypsinized to produce a single-cell suspension, washed in ice-cold PBS and resuspended in 0.7% low melting point agar (Quantum Biotechnologies Inc., Canada) in PBS at a concentration of 5×10^4 cells/ml. 150 μl of this suspension were pipetted onto precoated glass slides and then covered with a cover glass, and the agar was allowed to set at 4 °C. The sample was then placed in lysing solution. In the modified comet assay, the sample slide was washed in enzyme reaction buffer (40 mM HEPES, 0.1 M KCl, 0.5 mM EDTA, 0.2 mg/ml BSA, pH 8.0 with KOH) after the same process. This slide was treated with FPG (100 μl) for 30 min at 37 °C and with Endo III (100 μl) for 45 min at 37 °C and covered with a cover glass. The cells were washed in enzyme reaction buffer 3 times for 5 min. In the alkaline comet assay, cells were lysed in pH 10 lysis solution [2.5 M NaCl, 100 mM Na_2EDTA, 10 mM Tris–HCl, 1% Triton X-100, 10% (v/v) DMSO] at 4 °C for 60 min. The lysed cells and the cells in the modified comet assay were rinsed and allowed an unwinding time of 30 min in electrophoresis buffer (1 mM Na_2EDTA, 300 mM NaOH, pH > 13) before electrophoresis for 30 min at 25 V on ice. The gels were then neutralized with 0.4 M Tris–HCl (pH 7.5) for 10 min and stained with ethidium bromide (2 μg/ml) just prior to image analysis. DNA migration was assessed by fluorescence microscopy (Leica DMLB, excitation filter 515–560 nm and barrier filter of 590 nm) in conjunction with a digital camera. The images were evaluated by auto image analysis (Komet version 5.0; Kinetic Imaging Ltd., UK). The Olive Tail Moment (OTM; tail distance × percentage of DNA in tail) was used to quantify the DNA damage, based on the random scoring of 100 nuclei per slide. A minimum of two replicate comet slides were prepared for each sample.

2.6. In vitro micronucleus assay

With the Ag-NPs, we performed the MN assay with cytochalasin B (cytokinesis-block micronucleus, CBMN assay) and without cytochalasin B (MN assay) on the basis of the report that cytochalasin B affects MN formation [23]. The cells were seeded onto 8-well chamber slides at a density of 1.25×10^4 cells/well and cultured for 24 h until they reached 60–70% confluence. The treatment medium for BEAS-2B cells was prepared by adding 4 doses of Ag-NPs only or Ag-NPs with scavengers (Man 0.5 μM, SS 1 μg/ml, CAT 2 units/ml and SOD 30 units/ml) to growth medium in the absence or presence of 3 μg/ml cytochalasin B for 24 h [19–22]. The slides were washed twice with the same amount of PBS and left for 5 min at 4 °C after adding 1% trisodium citrate. The slides were then placed in fresh fixative (99:1 = methanol:acetic acid) at 4 °C, left on a clean bench to air-dry, and then placed in ribonuclease A (10 μg/ml in 2× SSC) for 6 min at 30 °C. The slides were rinsed in 2× SSC (0.03 M trisodium citrate, 0.3 M NaCl) and left on a clean bench to air-dry. After drying thoroughly, the slides were stained with 5% Giemsa solution for 5 h. Based on the MN scoring criterion, a score of 1000 binucleate cells per independent culture was obtained.

2.7. Oxidative stress assay

Cellular oxidative stress response was determined by monitoring ROS in the fluorescent DCF assay. Fluorescence increased when H_2DCF-DA (2′,7′-dichlorodihydrofluorescein-diacetate, Molecular Probe) was oxidized by ROS to DCF (2′,7′-dichlorofluorescein). This assay was carried out in BEAS-2B cells as described by Hussain et al. [1] and Schmid et al. [17]. The cells were harvested with 0.05% trypsin–0.53 mM EDTA·4Na (Gibco) and resuspended in BEGM. They were then seeded into 48-well plates at an initial concentration of 20×10^4 cells/well and allowed to attach for 24 h. In each case, the Ag-NPs solution (final concentration from 0.01 μg/ml to 10 μg/ml) was added to BEGM and incubated for 24 h. After incubation, each well was treated with H_2DCF (10 μM) for 1 h at 37 °C, then washed twice with serum-free medium and lysed using 0.1 N NaOH. The solution in each well was moved onto a white plate in order to measure the enzyme activity by fluorometer. DCF production was measured in a fluorometer (PerkinElmer, LS50B) with an excitation wavelength of 485 nm and an emission wavelength of 535 nm.

2.8. Data analysis

Sigma Plot 10.0 (Jandel Science Software, San Rafael, CA) and Excel 2007 (Microsoft, Redmond, WA) were used to analyze the data. The data from each assay were expressed as mean ± standard deviation. Statistical analysis was performed using SPSS (version 18.0, SPSS Inc., Chicago, IL). The Shapiro–Wilk test and Levene's test were used to evaluate normal distribution and homogeneity of variances, respectively. Differences between groups were tested by Duncan's post hoc test following one-way analysis of variance (ANOVA). Statistical significance was accepted at $p < 0.05$.

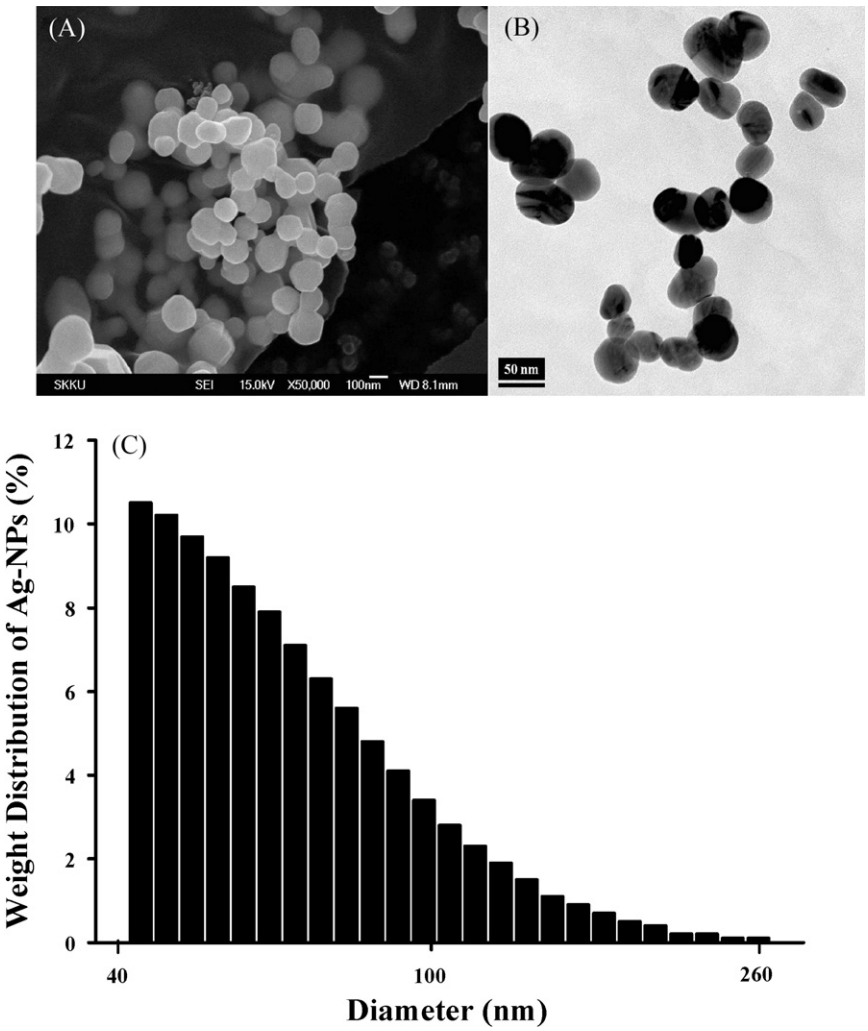

Fig. 1. Characterization of Ag-NPs using SEM (scanning electron microscope, A); TEM (transmission electron microscope, B); DLS (dynamic light scattering, C).

3. Results

3.1. Characterization and intracellular localization of Ag-NPs

In genotoxicity studies, Ag-NPs were characterized by SEM, TEM, and DLS, which showed spherical aggregates that were about 58.9 nm in size (Fig. 1). In SEM and TEM analysis, the single particle size of Ag-NPs was 100 nm or less (Fig. 1A and B), while the size distribution of Ag-NPs by DLS ranged from 43 to 260 nm (Fig. 1C). As shown in Fig. 2B and C, they existed as aggregates wrapped with an endocytic vesicle within the cytoplasm and nucleus of BEAS-2B cells that were treated with Ag-NPs for 24 h.

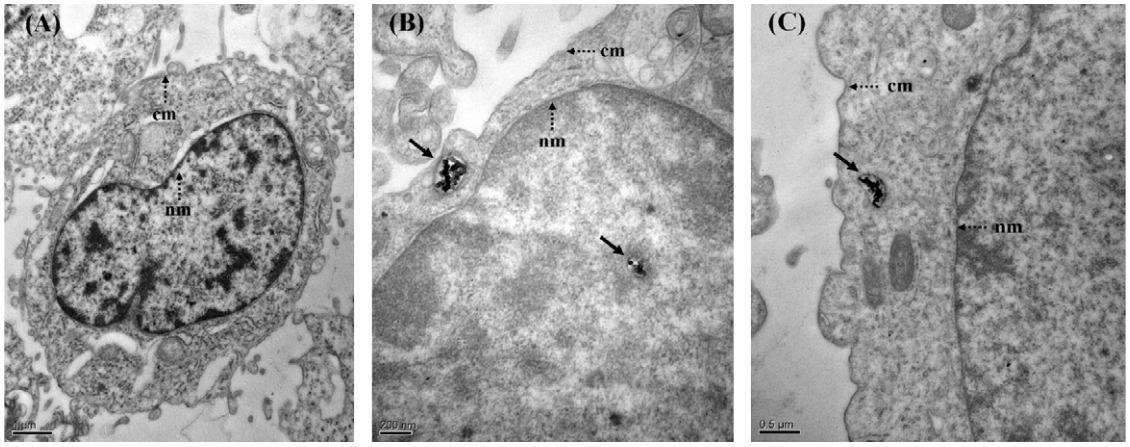

Fig. 2. TEM images of 80 nm sections of BEAS-2B cells treated with Ag-NPs. Ag-NPs are visible in the cells as black and electron-dense spots indicated by arrows. Dotted arrows show the cytoplasmic membrane (cm) and nuclear membrane (nm). Panel A is a representative image of untreated controls, and panels B and C are representative images of cells treated with 10 μg/ml of Ag-NPs for 24 h. Scale bars represent 1 μm in panel A, 200 nm in panel B, and 0.5 μm in panel C.

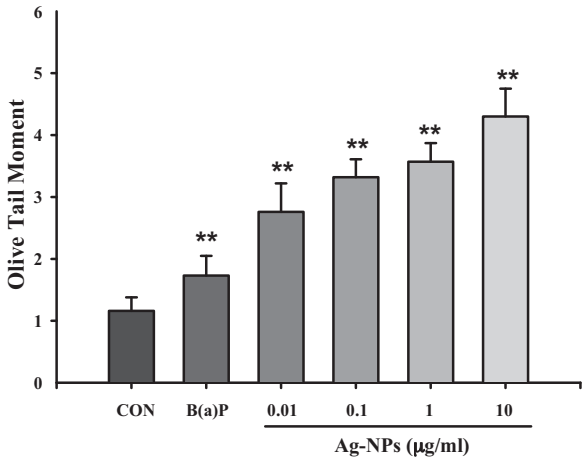

Fig. 3. DNA strand breaks in BEAS-2B cells exposed to Ag-NPs, as determined by comet assay. Cells were treated with 0.01–10 μg/ml of Ag-NPs or with B(a)P (benzopyrene, 10 μM) as a positive control. The results are expressed as the mean ± S.D. of three separate experiments for each data point of the olive tail moment (% DNA in tail × distance between centers of mass). Values are significantly different from control: $^{**}p < 0.01$.

3.2. The genotoxicity of Ag-NPs in BEAS-2B cells

We carried out all genotoxicity tests in BEAS-2B cells treated with Ag-NPs at non-cytotoxic concentrations (data not shown). In the comet assay, BEAS-2B cells treated with Ag-NPs exhibited a dose-dependent increase of DNA breakage (Fig. 3). The results of the CBMN and MN assays are shown in Fig. 4. The number of MN scored per 1000 binucleated cells increased in a dose-dependent manner in Fig. 4. In the CBMN assay, significant MN formation was also observed in cells treated with MMS (3.1-fold) and Ag-NPs (2.8-fold) compared with the control (Fig. 4A). In the MN assay without cytochalasin B, the MN formation was significantly induced by MMS (50 μg/ml; 3.0-fold) and Ag-NPs (10 μg/ml; 4.6-fold) compared with the control (Fig. 4B).

3.3. ROS generation

The fluorescent dye DCFH-DA was used to measure intracellular ROS generation by Ag-NPs in BEAS-2B cells. Hydrogen peroxide (H_2O_2; 50 μg/ml) was used as a positive control in BEAS-2B cells and increased the ROS generation by 2.68-fold. DCF fluorescence intensity was significantly increased by the Ag-NPs (0.01–10 μg/ml) after 24 h exposure, and ROS generation in cells treated with Ag-NPs (10 μg/ml) was 2.24-fold greater than that in the control (Fig. 5). This result confirms that exposure to Ag-NPs induced the generation of ROS.

3.4. Oxidative damage by Ag-NPs

In order to identify the oxidative DNA damage induced by Ag-NPs treatment, two repair-specific enzymes (FPG and ENDO III) that recognize and cut oxidized DNA bases were employed. Oxidative DNA damage was calculated by deducting OTM buffer from OTM enzymes, either in exposed or unexposed cells (Fig. 6). Post-treatment with FPG or ENDOIII significantly increased the DNA-damaging effects of AgNPs compared to FPG or ENDOIII control groups. In addition, FPG-treated cells showed greater oxidative DNA damage than ENDO III-treated cells (FPG: $^{**}p < 0.01$; ENDO III: $^{*}p < 0.05$). These results indicate that ROS generated by Ag-NPs increased the oxidative DNA damage, including oxidation of purines and pyrimidines; more significant oxidative damage was observed on purines in this study.

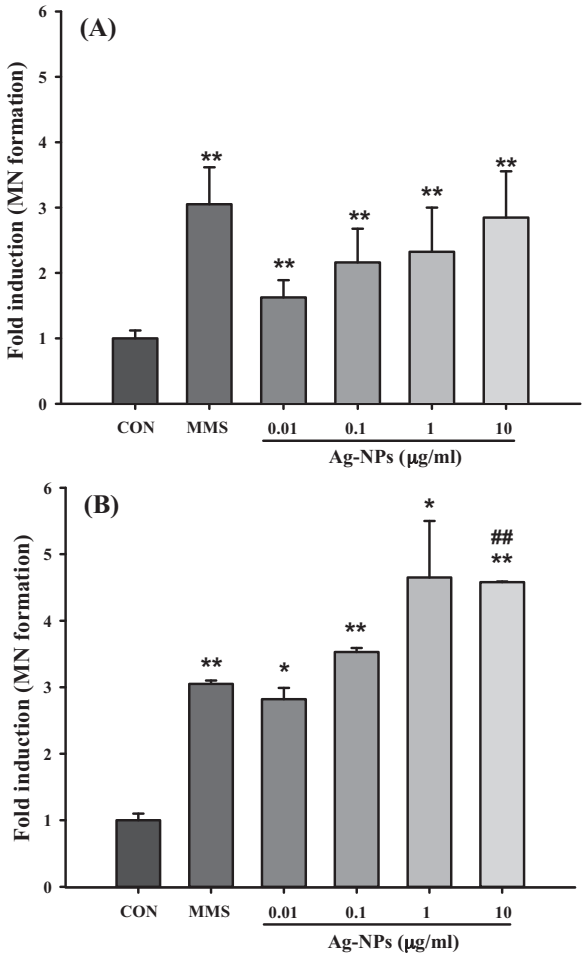

Fig. 4. Micronucleus formation induced by silver nanoparticles in BEAS-2B cells in the presence or absence of cytochalasin B. Cells were treated with Ag-NPs (0.01–10 μg/ml) in the presence (A) or absence (B) of cytochalasin B, or with the positive control, MMS (methyl methane sulfonate, 50 μg/ml). The assays were carried out as described in Section 2. The results are expressed as means ± S.D. of three separate experiments for each data point of MN frequency per 1000 cells. MN frequencies per 1000 cells of CON are (A) 9.9 ± 1.2 and (B) 6.8 ± 4.2, respectively. Values are significantly different from control: $^{**}p < 0.01$, $^{*}p < 0.05$; and higher than MMS: $^{\#\#}p < 0.01$.

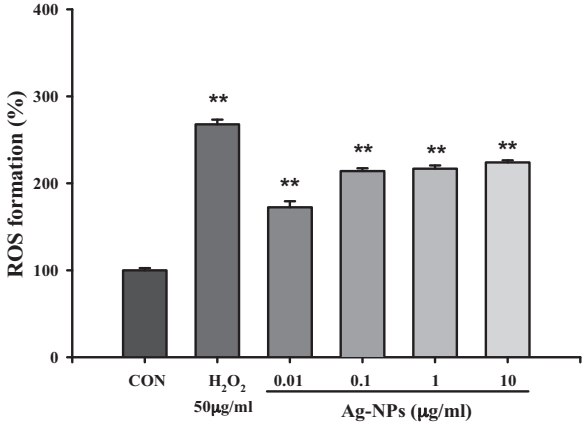

Fig. 5. Effect of Ag-NPs on ROS generation in BEAS-2B cells. Cells were seeded in 48-well plates and treated with 0.01, 0.1, 1 and 10 μg/ml for 24 h at 37 °C. ROS were detected by fluorescence measurement of DCF and the result is given in % control. The data are expressed as mean ± S.D. and compared to controls. Values are significantly different from control: $^{**}p < 0.01$.

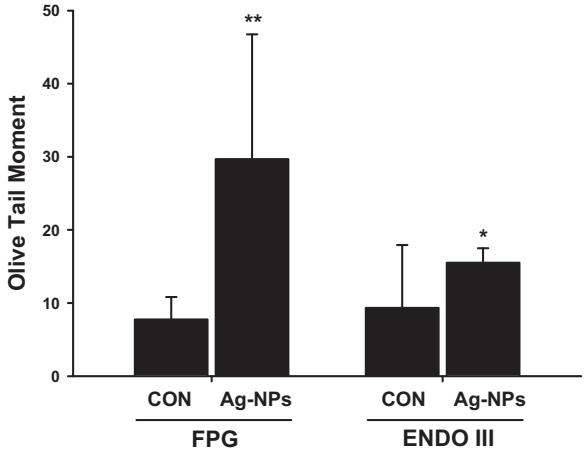

Fig. 6. The effects of FPG or ENDO III post-treatment on DNA breakage induced by Ag-NPs (10 μg/ml) in BEAS-2B cells (FPG: formamidopyrimidine DNA glycosylase; ENDO III: endonuclease III). The assays were carried out as described in Section 2. The bars are related to mean values of differences (OTM (olive tail moment) of cells treated with enzymes – OTM buffer) ± S.D. indicating oxidative DNA damage. The experiments were performed in triplicate. Values are significantly different from control: $^{*}p < 0.05$, $^{**}p < 0.01$.

The BEAS-2B cells were co-treated with Ag-NPs (10 μg/ml) and scavengers in the CBMN assay and comet assay (Fig. 7). In the CBMN assay, MN formation stimulated by Ag-NPs was significantly decreased by Man, SS, CAT, and SOD (Fig. 7A). The results demonstrated that SOD most effectively decreased MN formation, even though its effects were not statistically different from those of other scavengers. In the comet assay, DNA breakage induced by Ag-NPs (10 μg/ml) was significantly blocked by Man, SS, CAT and SOD. In particular, SOD exhibited a statistically (Duncan post hoc test) significant blocking effect versus other scavengers (Man, SS and CAT) (Fig. 7B) in comet assay.

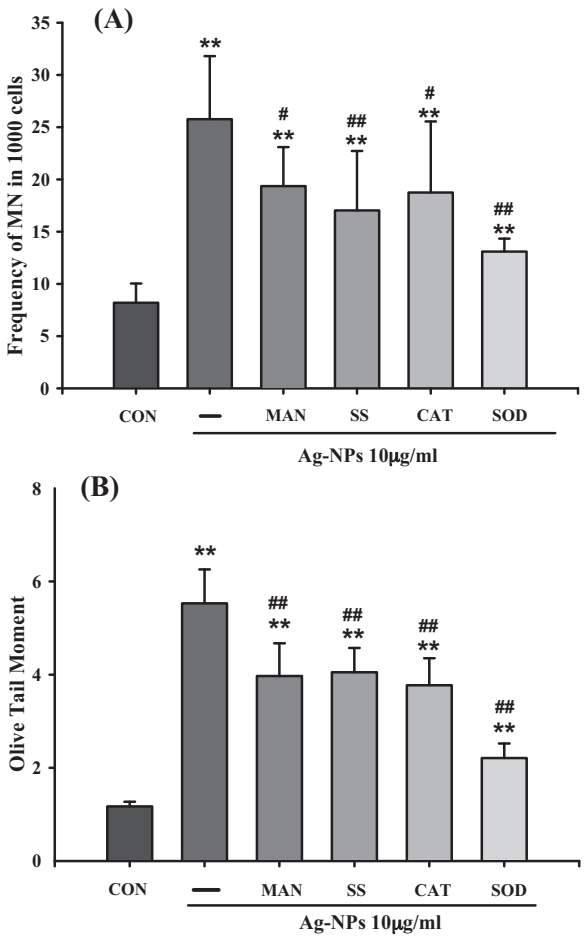

Fig. 7. DNA strand breaks and MN formation in BEAS-2B cells exposed to Ag-NPs as determined by CBMN assay and comet assay. Cells were treated with Ag-NPs (10 μg/ml) and with scavenging agents for 24 h at 37 °C (Man: mannitol; SS: sodium selenite; CAT: catalase; SOD: superoxide dismutase). The assays were carried out as described in Section 2. The results of the CBMN assay (A) are expressed as means ± S.D. of three separate experiments for each data point of MN frequency per 1000 cells. The results of the comet assay (B) are expressed as means ± S.D. of three separate experiments for each data point of the olive tail moment (% DNA in tail × distance between centers of mass). Values are significantly different from control: $^{**}p < 0.01$ and Ag-NPs 10 μg/ml: $^{\#}p < 0.05$, $^{\#\#}p < 0.01$.

4. Discussion

There are no standardized testing methods for the genotoxicity of nanoparticles [24,25]. In the review by Landsiedel et al. [25], the comet assay and MN assay were more sensitive and frequently used to confirm the genotoxicity of nanoparticles than the well-known Ames test in bacterial systems. The Ames tests on nanoparticles (e.g., TiO_2, ZnO, SWCNT) were predominantly negative, possibly due to penetration problems of the nanoparticles through the bacterial cell wall [25]. Therefore, penetration into the cell membrane is one of the key features in order for nanoparticles to induce genotoxic effects. Many researchers have suggested that size is a critical factor for nanoparticle-induced toxicity and biological responses [7,26–29]. Jiang et al. [28] reported that the sizes at which gold and silver nanoparticles exhibit the greatest cellular responses are 40 and 50 nm. According to this report, it is likely because such nanoparticles have a high chance of being taken up through endocytosis. Based on these studies, we first identified the size of the nanoparticles.

Ag nanopowder was purchased from Sigma–Aldrich [30–34], and Ag-NPs dispersed into culture medium were used for *in vitro* tests. In SEM and TEM analysis, the single particle size of Ag-NPs was 100 nm or less, but aggregates were also observed (Fig. 1A and B). The size distribution of Ag-NPs by DLS ranged from 43 to 260 nm (Fig. 1C), which could indicate that Ag-NPs clustered together and formed large agglomerated particles [27]. Despite aggregation of Ag-NPs, 40–59 nm nanoparticles accounted for approximately 50% (Fig. 1C), which should induce cellular responses according to Jiang's report.

Nanoparticles seem to differ from larger particles in the mechanisms of cellular uptake and localization. Geiser et al. [35] reported that ultrafine particles may be taken up into cells by diffusion via pores or adhesive interactions rather than by endocytic uptake. On the other hand, nano-sized fullerene may become compartmentalized within cells by phagocytosis of larger aggregates or by endocytosis [36]. In this study, the BEAS-2B cells were exposed to Ag-NPs for 24 h and we identified the intracellular localization of the Ag-NPs. Aggregated Ag-NPs were observed in endocytic vesicles within the cytoplasm and nucleus (Fig. 2B and C). These results indicate that uptake of Ag-NPs into cells may involve an endocytic pathway.

We conducted comet assay and MN assay as conventional testing methods [25] to confirm the genotoxicity of the Ag-NPs in BEAS-2B cells. The Ag-NPs induced dose-dependent DNA breakage in the comet assay (Fig. 3). In the CBMN and MN assay, Ag-NPs also stimulated a significant and dose-dependent increase of MN formation (Fig. 4). The MN formation in the presence of cytochalasin B was significantly induced by MMS (50 μg/ml; 3.1-fold) and Ag-NPs (10 μg/ml; 2.8-fold) compared with the control (Fig. 4A). A test compound is classified as a clastogen when it is able to enhance the spontaneous MN frequency by 3-fold or more over that of the

control for at least one dose tested [37,38]. Based on that criterion, the CBMN data was not sufficient to classify the Ag-NPs as a clastogen because induction was enhanced by less than 3-fold. However, we should consider the reports that cytochalasin B itself could interfere with the uptake of particles. Papageorgiou et al. [23] reported that micronuclei induction of microparticles was increased in the absence of cytochalasin B, an agent known to reduce phagocytosis [39,40]. Uptake of microparticles by phagocytosis was reported to play an important role in the DNA-damaging process. In bio-TEM image analysis, we found endocytic vesicles of Ag-NPs in the cytoplasm and nucleus of BEAS-2B cells exposed to Ag-NPs (Fig. 2). In addition, the MN formation in the absence of cytochalasin B was significantly induced by Ag-NPs (10 μg/ml; 4.6-fold) compared with the control (Fig. 4B). MN formation in the MN assay was greater than that in the CBMN assay. These results indicate that interference by cytochalasin B in the phagocytogenic uptake of Ag-NPs partially decreased the MN formation. Therefore, we suggest that Ag-NPs can be classified as clastogens and that phagocytosis may play an important role in the genotoxic effects of Ag-NPs.

We identified *in vitro* genotoxicity of Ag-NPs in human lung cells in this study. In addition, Kim et al. [41] reported that, in 90-day inhalation studies with Ag-NPs, inhalation exposure of Ag-NPs can induce changes in lung function, along with inflammation [13]. On the other hand, there is no report on the genotoxic effects of Ag-NPs in animal tissue, especially lung. For example, Kim et al. [41] did not find genotoxic effects in rat bone marrow in a 28-day oral study. Intrinsic toxic potential of nanoparticles should be determined using *in vitro* systems [42,43], in line with the tiered approach adopted in regulatory mammalian genotoxicity evaluations, before the toxicity of nanoparticles is determined using *in vivo* models. However, the *in vitro* toxic responses to Ag-NPs are not always predictive of *in vivo* pulmonary toxicities. For example, Sayes et al. [44,45] revealed very little correlation between *in vitro* and *in vivo* pulmonary toxicities of ZnO and fullerene. Although we concluded that Ag-NPs could be classified as clastogens, further genotoxicity studies in animal tissues are needed for more reliable risk assessment.

Many studies have demonstrated that nanoparticles (e.g., Ag-NPs and carbon nanotube) can generate ROS to a greater extent than larger particles [7,27]. In this study, we found that cells exposed to Ag-NPs showed a significant increase in ROS compared with control cells in the DCFH-DA assay (Fig. 5). In addition, Ag-NPs induced the oxidation of DNA bases, with more oxidation on purines than pyrimidines (Fig. 6). This result is consistent with reports that purines are the more vulnerable targets to oxidative DNA damage than pyrimidines, because the pyrimidines can be rapidly repaired by transferring an electron to their purine counterpart [46]. Furthermore, the genotoxic effect of Ag-NPs was partially blocked by scavengers (Fig. 7A and B). There are several studies on the plausible relationship between ROS generation of nanoparticles and endocytotic pathway. Carlson et al. [27] mentioned that size-dependent toxicity was caused by Ag-NPs and the predominant mechanism was largely mediated through oxidative stress in alveolar macrophages. This was confirmed in Nabeshi et al. [47], which showed that amorphous nanosilica induced endocytosis-dependent ROS generation and DNA damage in human keratinocytes by using cytochalasin D, an agent inhibiting endocytosis. From these studies, we concluded that Ag-NPs taken up by endocytosis might induce ROS generation and this stimulated genotoxic effects in human lung cells.

Particle-mediated oxidative stress may arise from mixed sources. Possible mechanisms for induction of oxidative stress by particles include direct generation of ROS from the surface of the particles, soluble compounds such as transition metals, and altered function of mitochondria or NADPH-oxidase [26]. Fullerene mediates the generation of various types of ROS through electron transfer to molecular oxygen, electron donor or acceptor [48], but the mechanisms of ROS generation by Ag-NPs are not yet clear. It was confirmed in the comet assay confirmed that SOD most significantly reduced the genotoxicity of Ag-NPs among the scavengers tested. In addition, as we could not find Ag-NPs in the mitochondria of cells in bio-TEM, we suggest that particle-related mitochondrial activation may not be the main toxicological route of Ag-NPs. Therefore, Ag-NPs may directly generate superoxide radical by activating membrane-bound NAD(P)H oxidase during uptake into cells and then secondarily generate the hydroxyl radical involved in the conversion of superoxide radical to hydrogen peroxide as previously reported by Boelsterli [49].

In summary, our *in vitro* studies demonstrate that the genotoxicity of Ag-NPs is related to ROS generation. Ag-NPs may generate superoxide radicals as they activate NAD(P)H oxidase in cells and then secondarily generate the hydroxyl radical involved in the conversion of superoxide radical to hydrogen peroxide. However, their mechanism of action has not been fully elucidated. Therefore, further studies should focus on the mechanism of ROS generation depending on uptake pathways and genotoxic effects in animal tests *in vivo*.

Conflict of interest statement

None.

Acknowledgments

This study was supported by the Eco-Technopia-21 project of the Korea Ministry of the Environment and the National Research Foundation of Korea Grant funded by the Korean Government (MEST).

References

[1] S.M. Hussain, K.L. Hess, J.M. Gearhart, K.T. Geiss, J.J. Schlager, In vitro toxicity of nanoparticles in BRL 3A rat liver cells, Toxicol. In Vitro 19 (2005) 975–983.
[2] S.M. Moghimi, A.C. Hunter, J.C. Murray, Long-circulating and target-specific nanoparticles: theory to practice, Pharmacol. Rev. 53 (2001) 283–318.
[3] J. Panyam, V. Labhasetwar, Biodegradable nanoparticles for drug and gene delivery to cells and tissue, Adv. Drug Deliv. Rev. 55 (2003) 329–347.
[4] C.W. Lam, J.T. James, R. McCluskey, R.L. Hunter, Pulmonary toxicity of single-wall carbon nanotubes in mice 7 and 90 days after intratracheal instillation, Toxicol. Sci. 77 (2004) 126–134.
[5] S. Foley, C. Crowley, M. Smaihi, C. Bonfils, B.F. Erlanger, P. Seta, C. Larroque, Cellular localisation of a water-soluble fullerene derivative, Biochem. Biophys. Res. Commun. 294 (2002) 116–119.
[6] J.R. Gurr, A.S. Wang, C.H. Chen, K.Y. Jan, Ultrafine titanium dioxide particles in the absence of photoactivation can induce oxidative damage to human bronchial epithelial cells, Toxicology 213 (2005) 66–73.
[7] A. Nel, T. Xia, L. Mädler, N. Li, Toxic potential of materials at the nanolevel, Science 311 (2006) 622–627.
[8] X. Chen, H.J. Schluesener, Nanosilver: a nanoproduct in medical application, Toxicol. Lett. 176 (2008) 1–12.
[9] A. Nagy, G. Mestl, High temperature partial oxidation reactions over silver catalysts, Appl. Catal. A 188 (1999) 337–353.
[10] S.A. Blaser, M. Scheringer, M. Macleod, K. Hungerbuhler, Estimation of cumulative aquatic exposure and risk due to silver: contribution of nanofunctionalized plastics and textiles, Sci. Total Environ. 390 (2008) 396–409.
[11] K.L. Dreher, Health and environmental impact of nanotechnology: toxicological assessment of manufactured nanoparticles, Toxicol. Sci. 77 (2004) 3–5.
[12] J.H. Sung, J.H. Ji, J.D. Park, J.U. Yoon, D.S. Kim, K.S. Jeon, M.Y. Song, J. Jeong, B.S. Han, J.H. Han, Y.H. Chung, H.K. Chang, J.H. Lee, M.H. Cho, B.J. Kelman, I.J. Yu, Subchronic inhalation toxicity of silver nanoparticles, Toxicol. Sci. 108 (2008) 452–461.
[13] J.H. Sung, J.H. Ji, J.U. Yun, D.S. Kim, M.Y. Song, J. Jeong, B.S. Han, J.H. Han, Y.H. Chung, J. Kim, T.S. Kim, H.K. Chang, E.J. Lee, J.H. Lee, I.J. Yu, Lung function changes in Sprague-Dawley rats after prolonged inhalation exposure to silver nanoparticles, Inhal. Toxicol. 20 (2008) 567–574.
[14] V.K. Sharma, R.A. Yngard, Y. Lin, Silver nanoparticles: green synthesis and their antimicrobial activities, Adv. Colloid Interface Sci. 145 (2009) 83–96.
[15] S. Barillet, M.L. Jugan, M. Laye, Y. Leconte, N. Herlin-Boime, C. Reynaud, M. Carrière, In vitro evaluation of SiC nanoparticles impact on A549 pulmonary cells: cyto-, genotoxicity- and oxidative stress, Toxicol. Lett. 198 (2010) 324–330.

[16] S. Kim, J.E. Choi, J. Choi, K.H. Chung, K. Park, J. Yi, D.Y. Ryu, Oxidative stress-dependent toxicity of silver nanoparticles in human hepatoma cells, Toxicol. In Vitro 23 (2009) 1076–1084.
[17] M. Schmid, S. Zimmermann, H.F. Krug, B. Sures, Influence of platinum, palladium and rhodium as compared with cadmium, nickel and chromium on cell viability and oxidative stress in human bronchial epithelial cells, Environ. Int. 33 (2007) 385–390.
[18] N.P. Singh, M.T. McCoy, R.R. Tice, E.L. Schneider, A simple technique for quantitation of low level of DNA damage in individual cells, Exp. Cell Res. 175 (1988) 184–191.
[19] J.S. Beckman, R.L. Minor Jr., C.W. White, J.E. Repine, G.M. Rosen, B.A. Freeman, Superoxide dismutase and catalase conjugated to polyethylene glycol increases endothelial enzyme activity and oxidant resistance, J. Biol. Chem. 263 (1988) 6884–6892.
[20] B.A. Markey, S.H. Phan, J. Varani, U.S. Ryan, P.A. Ward, Inhibition of cytotoxicity by intracellular superoxide dismutase supplementation, Free Radic. Biol. Med. 9 (1990) 307–314.
[21] H.J. Chae, K.C. Ha, D.S. Kim, G.S. Cheung, Y.G. Kwak, H.M. Kim, Y.M. Kim, H.O. Pae, H.T. Chung, S.W. Chae, H.R. Kim, Catalase protects cardiomyocytes via its inhibition of nitric oxide synthesis, Nitric Oxide 14 (2006) 189–199.
[22] S.G. Han, V. Castranova, V. Vallyathan, Comparative cytotoxicity of cadmium and mercury in a human bronchial epithelial cell line (BEAS-2B) and its role in oxidative stress and induction of heat shock protein 70, J. Toxicol. Environ. Health A 70 (2007) 852–860.
[23] I. Papageorgiou, C. Brown, R. Schins, S. Singh, R. Newson, S. Davis, J. Fisher, E. Ingham, C.P. Case, The effect of nano- and micron-sized particles of cobalt–chromium alloy on human fibroblasts in vitro, Biomaterials 28 (2007) 2946–2958.
[24] N. Lubick, Risks of nanotechnology remain uncertain, Environ. Sci. Technol. 42 (2008) 1821–1824.
[25] R. Landsiedel, M.D. Kapp, M. Schulz, K. Wiench, F. Oesch, Genotoxicity investigations on nanomaterials: methods preparation and characterization of test material, potential artifacts and limitations – many questions, some answers, Mutat. Res. 681 (2009) 241–258.
[26] L. Risom, P. Møller, S. Loft, Oxidative stress-induced DNA damage by particulate air pollution, Mutat. Res. 592 (2005) 119–137.
[27] C. Carlson, S.M. Hussain, A.M. Schrand, L.K. Braydich-stolle, K.L. Hess, R.L. Jones, J.J. Schlager, Unique cellular interaction of silver nanoparticles: size-dependent generation of reactive oxygen species, J. Phys. Chem. B 112 (2008) 13608–13619.
[28] W. Jiang, B.Y. Kim, J.T. Rutka, W.C. Chan, Nanoparticle-mediated cellular response is size-dependent, Nat. Nanotechnol. 3 (2008) 145–150.
[29] G. Jia, H. Wang, L. Yan, X. Wang, R. Pei, T. Yan, Y. Zhao, X. Guo, Cytotoxicity of carbon nanomaterials: single-wall nanotube multi-wall nanotube, and fullerene, Environ. Sci. Technol. 39 (2005) 1378–1383.
[30] D. Chen, T. Xi, J. Bai, Biological effects induced by nanosilver particles: in vivo study, Biomed. Mater. 2 (2007) S126–S128.
[31] J. Tang, L. Xiong, S. Wang, J. Wang, L. Liu, J. Li, Z. Wan, T. Xi, Influence of silver nanoparticles on neurons and blood–bain barrier via subcutaneous injection in rats, Appl. Surf. Sci. 255 (2008) 502–504.
[32] J. Tang, L. Xiong, G. Zhou, S. Wang, J. Wang, L. Liu, J. Li, F. Yuan, S. Lu, Z. Wan, L. Chou, T. Xi, Silver nanoparticles crossing through and distribution in the blood–brain barrier in vitro, J. Nanosci. Nanotechnol. 10 (2010) 6313–6317.
[33] J.Y. Roh, S.J. Sim, J. Yi, K. Park, K.H. Chung, D.Y. Ryu, J. Choi, Ecotoxicity of silver nanoparticles on the soil nematode Caenorhabditis elegans using functional ecotoxicogenomics, Environ. Sci. Technol. 43 (2009) 3933–3940.
[34] G. Laban, L.F. Nies, R.F. Turco, J.W. Bickham, M.S. Sepúlveda, The effects of silver nanoparticles on fathead minnow (Pimephales promelas) embryos, Ecotoxicology 19 (2010) 185–195.
[35] M. Geiser, B. Rothen-Rutishauser, N. Kapp, S. Schürch, W. Kreyling, H. Schulz, M. Semmler, V. Im Hof, J. Heyder, P. Gehr, Ultrafine particles cross cellular membrane by nonphagocytic mechanisms in lungs and cultured cells, Environ. Health Perspect. 113 (2005) 1555–1560.
[36] A.E. Porter, K. Muller, J. Skepper, P. Midgley, M. Welland, Uptake of C60 by human monocyte macrophages, its localization and implications for toxicity: studied by high resolution electron microscopy and electron tomography, Acta Biomater. 2 (2006) 409–419.
[37] M. Fenech, The cytokinesis-block micronucleus technique: a detailed description of the method and its application to genotoxicity studies in human populations, Mutat. Res. 285 (1993) 35–44.
[38] B.M. Miller, E. Pujadas, E. Gocke, Evaluation of the micronucleus test in vitro using Chinese hamster cells: results of four chemicals weakly positive in the in vivo micronucleus test, Environ. Mol. Mutagen. 26 (1995) 240–247.
[39] K. Murai, K. Tsunewaki, Photoperiod-sensitive cytoplasmic male sterility in wheat with Aegilops crassa cytoplasm, Euphytica 67 (1993) 41–48.
[40] P. Haynes, T.R. Lambert, I.D. Mitchell, Comparative in vivo genotoxicity of antiviral nucleoside analogues; penciclovir, acyclovir, ganciclovir and the xanthine analogue, caffeine, in the mouse bone marrow micronucleus assay, Mutat. Res. 369 (1996) 65–74.
[41] Y.S. Kim, J.S. Kim, H.S. Cho, D.S. Rha, J.M. Kim, J.D. Park, B.S. Choi, R. Lim, H.K. Chang, Y.H. Chung, I.H. Kwon, J. Jeong, B.S. Han, I.J. Yu, Twenty eight-day oral toxicity, genotoxicity, and gender-related tissue distribution of silver nanoparticles in Sprague-Dawley rats, Inhal. Toxicol. 20 (2008) 575–583.
[42] D.R. Dixon, A.M. Pruski, L.R. Dixon, A.N. Jha, Marine invertebrate eco-genotoxicology: a methodological overview, Mutagenesis 17 (2002) 495–507.
[43] A.N. Jha, Genotoxicological studies in aquatic organisms: an overview, Mutat. Res. 552 (2004) 1–17.
[44] C.M. Sayes, A.A. Marchione, K.L. Reed, D.B. Warheit, Comparative pulmonary toxicity assessments of C60 water suspensions in rats: few differences in fullerene toxicity in vivo in contrast to in vitro profiles, Nano Lett. 7 (2007) 2399–2406.
[45] C.M. Sayes, K.L. Reed, D.B. Warheit, Assessing toxicity of fine and nanoparticles: comparing in vitro measurements to in vivo pulmonary toxicity profiles, Toxicol. Sci. 97 (2007) 163–180.
[46] S.V. Jovanovic, M.G. Simic, One-electron redox potentials of purines and pyrimidines, J. Phys. Chem. 90 (1986) 974–978.
[47] H. Nabeshi, T. Yoshikawa, K. Matsuyama, Y. Nakazato, S. Tochigi, S. Kondoh, T. Hirai, T. Akase, K. Nagano, Y. Abe, Y. Yoshioka, H. Kamada, N. Itoh, S. Tsunoda, Y. Tsutsumi, Amorphous nanosilica induce endocytosis-dependent ROS generation and DNA damage in human keratinocytes, Part. Fibre Toxicol. 8 (2011) 1–10.
[48] Z. Markovic, V. Trajkovic, Biomedical potential of the reactive oxygen species generation and quenching by fullerenes (C60), Biomaterials 29 (2008) 3561–3573.
[49] U.A. Boelsterli, Mechanistic Toxicology: The Molecular Basis of How Chemicals Disrupt Biological Targets, Taylor & Francis, London, 2003.